

Motor neuron columnar fate imposed by sequential phases of Hox-c activity

Jeremy S. Dasen¹, Jeh-Ping Liu² & Thomas M. Jessell¹

¹Howard Hughes Medical Institute, Department of Biochemistry and Molecular Biophysics, Center for Neurobiology and Behavior, Columbia University, 701 West 168th Street, New York, New York 10032, USA

²University of Virginia School of Medicine, Department of Neuroscience, Lane Road extended, MR4, Room 5032, Charlottesville, Virginia 22908, USA

The organization of neurons into columns is a prominent feature of central nervous system structure and function. In many regions of the central nervous system the grouping of neurons into columns links cell-body position to axonal trajectory, thus contributing to the establishment of topographic neural maps. This link is prominent in the developing spinal cord, where columnar sets of motor neurons innervate distinct targets in the periphery. We show here that sequential phases of Hox-c protein expression and activity control the columnar differentiation of spinal motor neurons. Hox expression in neural progenitors is established by graded fibroblast growth factor signalling and translated into a distinct motor neuron Hox pattern. Motor neuron columnar fate then emerges through cell autonomous repressor and activator functions of Hox proteins. Hox proteins also direct the expression of genes that establish motor topographic projections, thus implicating Hox proteins as critical determinants of spinal motor neuron identity and organization.

Columns are basic units of neuronal organization in the vertebrate central nervous system (CNS)^{1,2}, but the mechanisms that control their assembly remain unclear. One region of the CNS in which neuronal columnar organization has been studied intensively is the spinal cord, where distinct columnar subtypes of motor neurons are known to innervate different muscle and neuronal targets in the periphery³. All spinal motor neurons (MNs) derive from progenitor cells located at a constant dorso-ventral position in the neural tube⁴, but motor neurons appear to acquire their discrete columnar identities as a function of position along the rostrocaudal axis of the spinal cord^{5–8} (Supplementary Fig. S1a–c). Limb levels of the spinal cord generate lateral motor column (LMC) neurons, whereas intervening thoracic levels give rise to autonomic MNs (termed Column of Terni (CT) neurons in chick)^{5–8}. Along the dorsoventral axis, the graded signalling activity of Sonic hedgehog (Shh) determines the position of MN generation by regulating the spatial expression of a set of homeodomain transcription factors within neural progenitors^{4,9}. The constancy of Shh signalling along the rostrocaudal axis, however, implies that other signalling pathways control the diversification of MNs into distinct columnar subtypes.

One source of signals that can influence the columnar fate of spinal motor neurons is the paraxial mesoderm. The transposition of paraxial mesoderm between limb and thoracic levels soon after neural tube closure results in the respecification of LMC and CT identity, and a similar switch in columnar fates is observed after transposition of the neural tube¹⁰. However, before neural tube closure, signals from axial mesodermal tissues—the node and nascent notochord—have been shown to regulate the molecular identity of MNs along the rostrocaudal axis of the spinal cord¹¹. In particular, members of the Hox-c homeodomain protein cluster are expressed by post-mitotic MNs generated at distinct rostrocaudal positions¹¹, and profiles of Hox-c protein expression characteristic of brachial, thoracic and lumbar MNs can be induced *in vitro* by early exposure of neural cells to increasing levels of fibroblast growth factor (FGF) signalling^{11,12}. Moreover, the pattern of Hox-c protein expression changes along with columnar identity after early transposition of brachial and thoracic neural tube¹⁰. Hox proteins influence MN diversification in the hindbrain^{13–15}, and thus a role for Hox proteins in the assignment of spinal MN columnar identity is plausible. Nevertheless, the link between axial FGF signalling,

neural Hox protein expression, and the establishment of spinal MN columnar identity, if any, remains obscure.

Hox protein expression segregates with MN columnar subtype

To explore the link between Hox expression and MN columnar identity, we focused initially on Hox-c proteins, because members of this Hox cluster are prominently expressed by MNs¹¹. We examined how the expression of Hoxc5, Hoxc6, Hoxc8 and Hoxc9 at brachial and thoracic levels of the spinal cord is matched to the differentiation of LMC and CT neurons^{5,16}.

Hoxc6 expression by MNs (defined by Isl1/2 expression) was confined to brachial levels, whereas Hoxc9 expression by MNs was restricted to thoracic levels (Fig. 1a). Hoxc6⁺ and Hoxc9⁺ MNs were interspersed at the border of the brachial and thoracic spinal cord, but very few neurons expressed both proteins (Fig. 1a, g). The rostrocaudal domains of expression of Hoxc5 and Hoxc8 by MNs were also segregated (Fig. 1b, h), but in contrast to Hoxc6 and Hoxc9, the transition from Hoxc5⁺ to Hoxc8⁺ MNs mapped to the mid-brachial level (Fig. 1c; Supplementary Fig. S2c). Thus, rostral brachial LMC neurons co-express Hoxc5 and Hoxc6, whereas caudal brachial LMC neurons co-express Hoxc6 and Hoxc8 (Fig. 1c, e, f, i, k). At rostral thoracic levels, many MNs initially co-expressed Hoxc8 and Hoxc9 (Fig. 1d, j).

MN columnar subtypes located at different rostrocaudal positions can be delineated by LIM homeodomain transcription factor expression¹⁷. In addition, CT neurons can be distinguished by expression of *BMP5*, a transforming growth factor- β family member¹⁸, and LMC neurons by expression of retinaldehyde dehydrogenase-2 (RALDH2), a key enzyme in retinoic acid synthesis^{19,20} (Supplementary Fig. S1d). We therefore examined whether the profile of Hox-c protein expression by MNs corresponds to the position of newly generated brachial LMC neurons and of CT neurons. At brachial levels, the rostral and caudal boundaries of RALDH2 expression coincided closely with the domain of Hoxc6⁺, Hoxc9⁻ MNs (Fig. 1l, m, o; Supplementary Fig. S2a, b). At thoracic levels, the rostral and caudal boundaries of *BMP5* expression coincided with the domain of Hoxc9⁺, Hoxc6⁻ MNs (Fig. 1n–p; Supplementary Fig. S2d, e). Together, these data indicate that Hoxc6 and Hoxc9 expression within MNs coincides with brachial LMC and thoracic CT columns, respectively (Fig. 1q).

Regulation of Hox-c protein expression by FGF signalling

The exposure of neural progenitor cells *in vitro* to increasing FGF levels induces the differentiation of MNs with a progressively more caudal Hox-c profile, suggesting a model in which the positional identity of MNs at brachial and thoracic levels is established by graded FGF signalling¹¹.

To test this model *in vivo*, we examined whether an increase in the level of FGF signalling in the neural tube elicits a rostral to caudal switch in the profile of Hox-c protein expression. *In ovo* electroporation was used to co-express *FGF8* and the green fluorescent protein gene *GFP* (as an indicator of transfected cells) unilaterally in brachial and thoracic regions of the stage 12 neural tube (Fig. 2a). The concentration of *FGF8* plasmid was titrated to a level that did not perturb neural tube morphology or change the dorsoventral pattern of progenitor homeodomain proteins (see Methods). Expression of *FGF8* resulted in the extinction of *Hoxc6* expression and the onset of *Hoxc9* expression at brachial levels (Fig. 2b–f). Similarly, exposure of rostral brachial levels to *FGF8* led to the extinction of *Hoxc5* and to a rostral expansion in *Hoxc8* expression (Fig. 2g, h). Thus, brachial FGF expression results in a brachial to thoracic switch in the profile of Hox-c expression.

Because profiles of Hox-c protein expression characteristic of lumbar levels of the spinal cord can be induced by early exposure of neural cells to high level FGF signalling^{11,12}, we also examined whether the expression of *FGF8* at thoracic levels resulted in a switch to a lumbar Hox-c expression profile. However, *FGF8* expression did not markedly influence the profile Hox-c expression at thoracic levels (Supplementary Fig. S3a–e), a finding likely to reflect a comparatively low level of FGF8 signalling achieved under these electroporation conditions.

FGF signalling and the specification of MN columnar identity

We next examined whether increased FGF8 signalling in brachial

neural tube influences MN columnar identity. Brachial expression of *FGF8* did not suppress the generation of *Isl1/2*⁺ MNs, but reduced the total MN number by ~30% at stage 29 (Fig. 2i, j), a finding consistent with observations that the number of MNs generated at brachial levels of the spinal cord normally exceeds that at thoracic levels²⁰. The number of medial MMC neurons, assessed by *Lim3* expression¹⁷ was not altered (Supplementary Fig. S3i), consistent with the presence of this motor column at both brachial and thoracic levels.

After *FGF8* expression, however, brachial MNs lacked *RALDH2* expression (Fig. 2k). The expression of *RALDH2* by LMC neurons directs lateral LMC divisional identity, defined by co-expression of *Isl2* and *Lim1*¹⁷. Consistent with this, we detected a virtually complete loss of *Isl2*⁺, *Lim1*⁺ MNs (Fig. 2j). Thus, increased FGF8 signalling in brachial neural tube suppresses LMC differentiation in a manner that parallels the suppression of *Hoxc6* expression.

We examined whether the loss of LMC columnar identity is accompanied by the emergence of a thoracic programme of MN columnar differentiation. After brachial *FGF8* expression and analysis at stage 29, the characteristic ovoid clustering of MNs typical of the LMC was lost, and instead MNs were clustered in a semilunar arrangement, typical of thoracic MNs¹⁷ (Fig. 2j). Moreover, many brachial MNs now expressed the bone morphogenetic protein gene *BMP5* (Fig. 2l), indicating that they have acquired a CT identity. Analysis at stage 29 revealed that many *islet-1*⁺ (*Isl1*⁺), *BMP5*⁺ MNs had migrated to a dorsomedial position typical of CT neurons (Fig. 2j, Supplementary Fig. S3j). Thus, elevated brachial FGF8 signalling results in a conversion from LMC to CT columnar identity, paralleling the switch from *Hoxc6* to *Hoxc9* expression.

Several lines of evidence indicate that the brachial to thoracic switch in Hox-c expression and MN columnar identity results from a direct action of FGF8 on neural cells. Brachial neural expression of

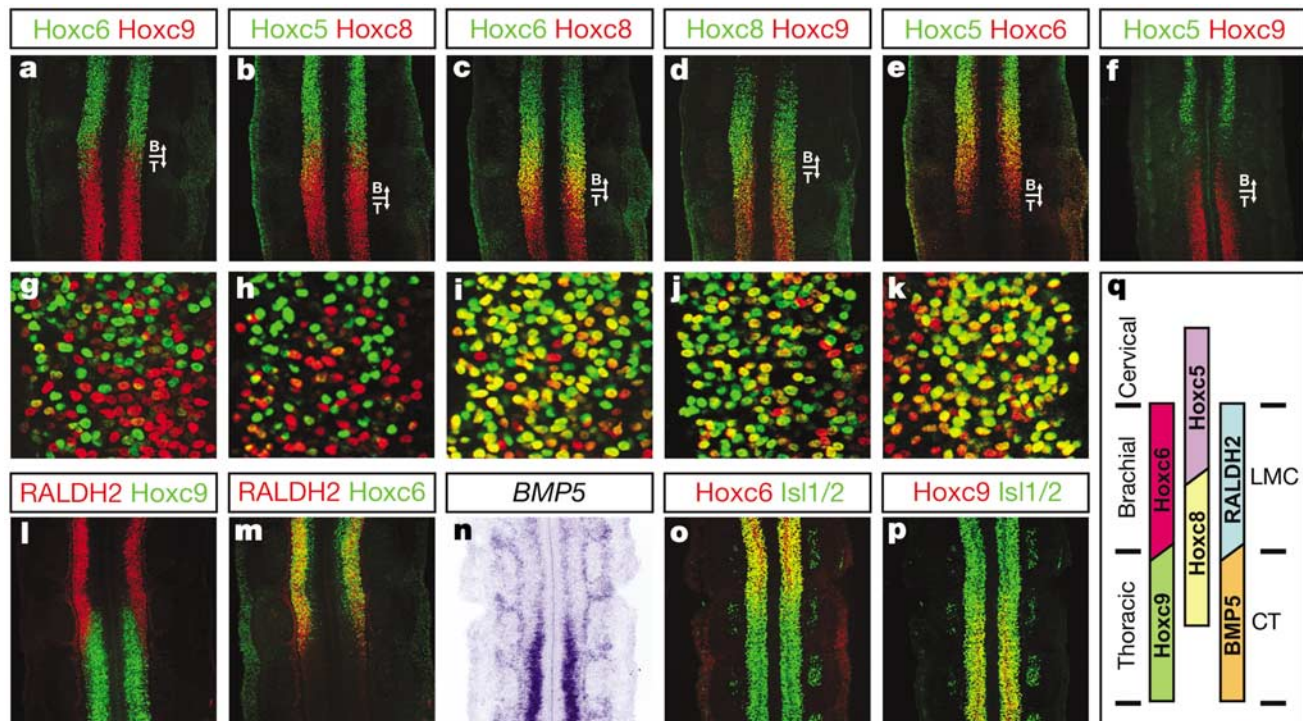


Figure 1 Hox-c protein expression and spinal motor neuron columnar identity. **a–f**, Hox5, Hox6, Hox8 and Hox9 protein expression in horizontal longitudinal sections of stage 24 brachial and thoracic chick spinal cord. T-junction indicates position of the brachial (B) and thoracic (T) border. **g–k**, Higher magnification images of Hox-c expression reveals few if any *Hoxc6*⁺/*Hoxc9*⁺ or *Hoxc5*⁺/*Hoxc8*⁺ neurons, but many

Hoxc6⁺/*Hoxc8*⁺, *Hoxc8*⁺/*Hoxc9*⁺, and *Hoxc5*⁺/*Hoxc6*⁺ neurons. **l–p**, Domains of Hox6 and Hox9 expression in stage 24 chick spinal cord, in comparison to *RALDH2*, *BMP5* and *Isl1/2* expression. **q**, Rostrocaudal domains of Hox5, Hox6, Hox8 and Hox9 expression in MNs, with respect to molecularly defined MN columns.

a constitutively active FGF type I receptor that functions in a cell-autonomous manner^{11,21} mimicked the actions of FGF8 in suppressing Hoxc6 and RALDH2 expression, and in inducing Hoxc9 and BMP5 expression¹¹ (Supplementary Fig. S4a–d). In addition, expression of FGF8 in brachial neural cells did not change the Hox-c profile of the adjacent paraxial mesoderm (data not shown). Moreover, the spatial extent of FGF8 signalling, revealed by di-phosphorylated mitogen-activated protein kinase (MAPK) (ERK1/2) expression²², appeared to be confined to neural cells (Supplementary Fig. S4e–g).

Specification of MN columnar identity by Hox-c proteins

If the FGF8-elicited switch from LMC to CT columnar fate is mediated by changes in Hox expression, then ectopic expression of individual Hox-c proteins might be expected to change MN columnar fate.

To test this idea, we expressed Hoxc9 in stage 12 brachial neural tube, using a CMV/ β -actin promoter (pCAGGS), and analysed changes in Hox-c expression and MN columnar identity at stages 27 to 29. Brachial expression of Hoxc9 inhibited Hoxc6 expression by MNs (Fig. 3a; <3% of MNs co-expressed Hoxc9 and Hoxc6). Moreover, the suppression of Hoxc6 expression was restricted to MNs that expressed Hoxc9 (Fig. 3a), indicating the cell-autonomy of Hoxc9 action. Brachial expression of Hoxc9 suppressed LMC differentiation in a cell-autonomous manner, as assessed by the loss

of RALDH2 expression (Fig. 3b, c), and also markedly reduced the number of Isl2⁺, Lim1⁺ lateral LMC neurons (Fig. 3d). Remarkably, many brachial Hoxc9⁺, Isl1/2⁺ MNs expressed BMP5 (Fig. 3f), and by stage 29, many Isl1⁺, Hoxc9⁺, BMP5⁺ MNs were located in a dorsomedial position, characteristic of CT neurons (Fig. 3e, g). Thus, brachial expression of Hoxc9 mimics the effects of increased FGF8 signalling, repressing Hoxc6 expression and LMC differentiation, and inducing CT identity.

We next examined whether thoracic Hoxc6 expression elicits a caudal to rostral switch in MN columnar identity. Thoracic Hoxc6 misexpression led to the cell-autonomous repression of Hoxc9 expression by MNs, prevented expression of BMP5, and inhibited the later dorsomedial migration of Isl1⁺ MNs (Fig. 3h–j and data not shown). In addition, many thoracic Hoxc6⁺ MNs acquired an LMC identity, assessed by RALDH2 expression, the presence of Isl2⁺, Lim1⁺ lateral LMC neurons, and by expression of Nkx6 proteins, additional markers of LMC neurons²³ (Fig. 3k–o). Forced expression of Hoxc6 or Hoxc9 within their normal segmental domains did not change the profile of MN columnar differentiation (data not shown). Together, these findings provide evidence that Hoxc6 and Hoxc9 specify, respectively, brachial LMC and thoracic CT identity. The corresponding Hox-a paralogues, Hoxa6 and Hoxa9, have similar expression patterns and MN columnar specification activities (Supplementary Figs S5a–d and S6a–e).

The activities of Hox6 and Hox9 proteins also appear selective.

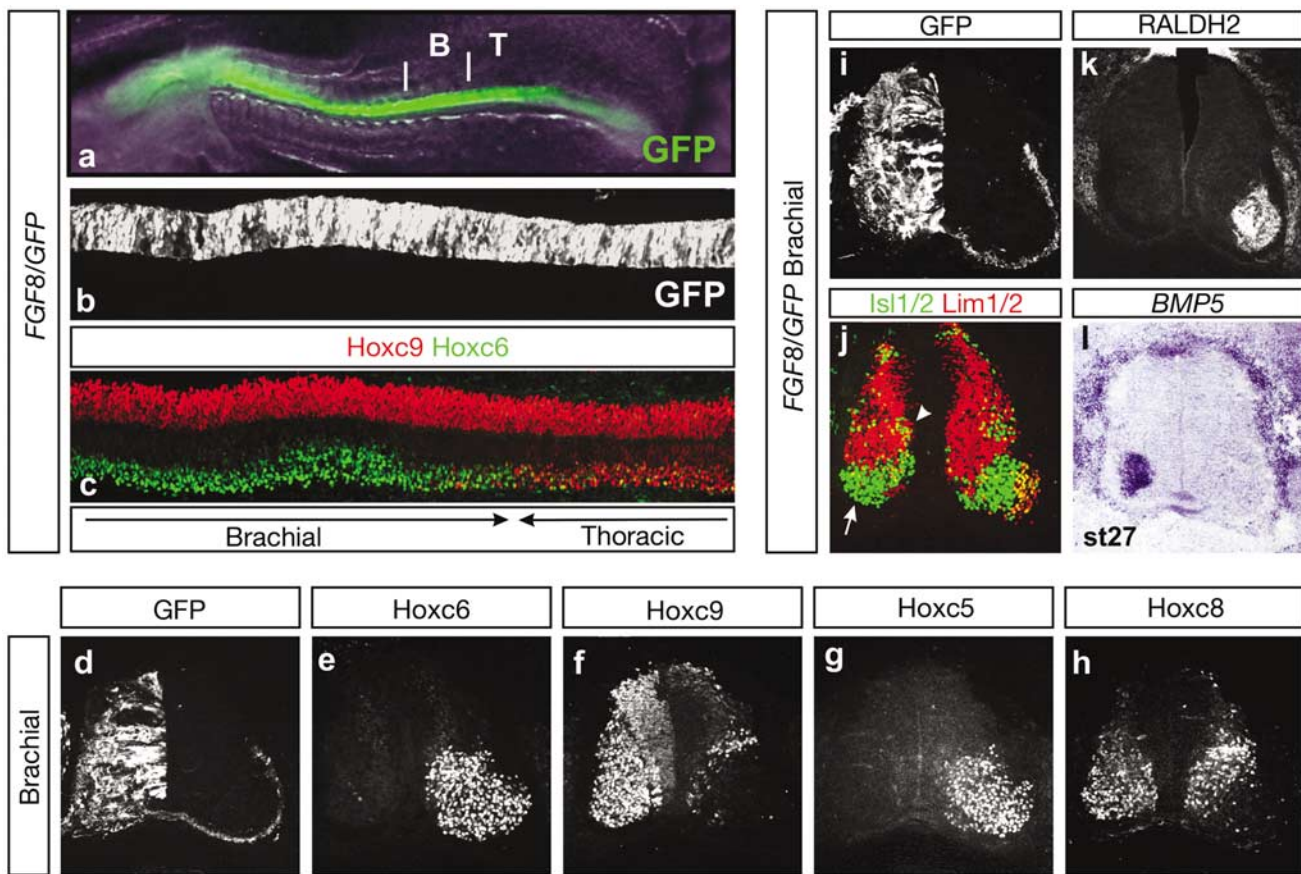


Figure 2 Hox-c and motor column repatterning after FGF8 expression in brachial neural tube. **a**, Top-down image of a chick embryo 8 h after unilateral co-electroporation of CMV-enhanced GFP and CMV-FGF8 expression plasmids at stage 12. GFP is expressed at brachial (B) and thoracic (T) levels. **b, c**, Top-down views of brachial and thoracic levels of a chick spinal cord, ~48 h after FGF8/GFP electroporation stage 12. **d–h**, Hox-c expression in cross-sections of stage 29 brachial spinal cord after FGF8/GFP electroporation. Ectopic expression of Hox-c proteins is detected in MNs and ventral

interneurons. Loss of Hoxc6 protein is accompanied by loss of Hoxc6 mRNA (see Supplementary Fig. S3k, l). **i–l**, MN columnar marker expression after brachial FGF8/GFP electroporation. The loss of lateral LMC neurons (arrow in Fig. 2j) is accompanied by the appearance of dorsomedially positioned Isl1⁺ MNs (arrowhead in Fig. 2j). **l**, BMP5 expression at stage 27 after brachial FGF8 electroporation. The differentiation of MN columnar subtypes was not markedly affected at thoracic levels of the spinal cord (Supplementary Fig. S3e–h).

Expression of *Hoxc6* at rostral thoracic levels failed to suppress *Hoxc8* and conversely, ectopic expression of *Hoxc8* at rostral brachial levels did not suppress *Hoxc6* or *RALDH2* expression (Supplementary Fig. S6f–i). In contrast, expression of *Hoxc8* at rostral brachial levels suppressed *Hoxc5* expression (Supplementary Fig. S6j), providing evidence that the exclusive domains of expression of *Hoxc5* and *Hoxc8* within the LMC are also established by selective cross-repressive interactions.

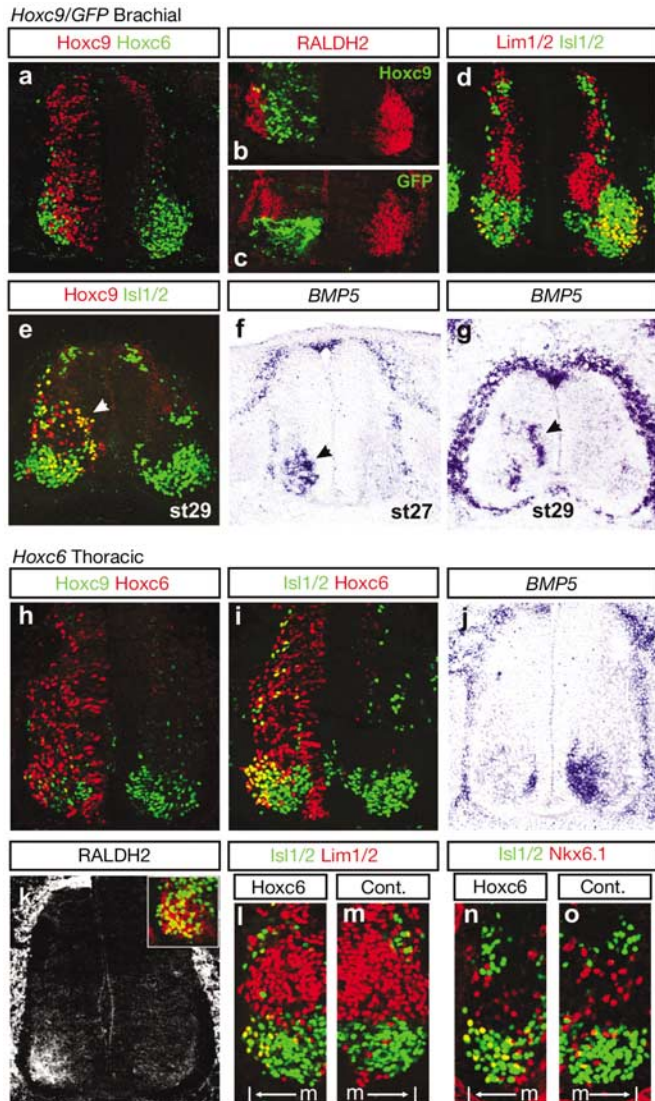


Figure 3 Motor columnar patterning activities of *Hoxc9* and *Hoxc6*. **a**, Pattern of *Hoxc6* after expression of chick *Hoxc9* in stage 12 brachial neural tube, and analysis at stage 27. **b–d**, Pattern of *RALDH2* expression and reduction in the number of *Isl2*⁺, *Lim1*⁺ lateral LMC MNs after brachial expression of *Hoxc9* GFP. **e**, Dorsomedial position of *Hoxc9*⁺, *Isl1*⁺ MNs (white arrowhead) after *Hoxc9* expression. **f, g**, Induction of *BMP5* expression in premigratory (stage 27) and dorsomedially positioned (stage 29) MNs (black arrowhead). **h**, Expression of *Hoxc9* after thoracic expression of murine *Hoxc6* in stage 12 neural tube. **i**, *Hoxc6*⁺/*Isl1*⁺ MNs settle in a ventrolateral position. **j**, *BMP5* expression after thoracic *Hoxc6* expression. **k**, Induction of *RALDH2* expression in *Hoxc6*⁺ MNs. Inset shows co-expression of *Hoxc6* (green) and *RALDH2* (red). **l–o**, Expression of LMC markers after thoracic *Hoxc6* expression. Many *Isl1/2*⁺ MNs co-express *Lim1* (**l, m**) and *Nkx6.1* (**n, o**). Medial (m) and lateral (l) positions in the spinal cord are indicated. Medial MMC neurons at brachial and thoracic levels express *Hoxc6* and *Hoxc9*, respectively. At both levels some MNs retain a medial MMC identity, assessed by LIM homeodomain protein *Lim3* expression, after expression of the segmentally inappropriate Hox-c protein (data not shown). Cont., contralateral side.

Hox6 and Hox9 expression and regulation in neural progenitors

Does the profile of Hox expression in post-mitotic MNs emerge from an earlier rostrocaudal difference in *Hox6* and *Hox9* expression by neural progenitors? Expression of *Hox6* paralogues was absent from brachial progenitor cells between stages 10 to 14, whereas expression of *Hoxc6* messenger RNA was detected in thoracic progenitors (Supplementary Fig. S5e–g). *Hoxc6* protein, however, was not detected in thoracic progenitors (Fig. 4f). Expression of *Hoxa9*, *Hoxb9* and *Hoxc9* mRNA and *Hoxc9* protein was detected in thoracic neural progenitors at stage 15, just before the generation of post-mitotic MNs (Fig. 4a–c, e). Each *Hox9* gene was expressed over the same general domain, with a rostral limit of expression at somites 20/21 (Fig. 4a–c). Taken together, these findings indicate that brachial progenitors lack expression of *Hox6* and *Hox9* proteins, whereas thoracic progenitors express *Hox9* but not *Hox6* proteins (Fig. 4j).

We next examined whether FGF8 signalling changes the profile of *Hox* gene expression in neural progenitors. After brachial *FGF8*

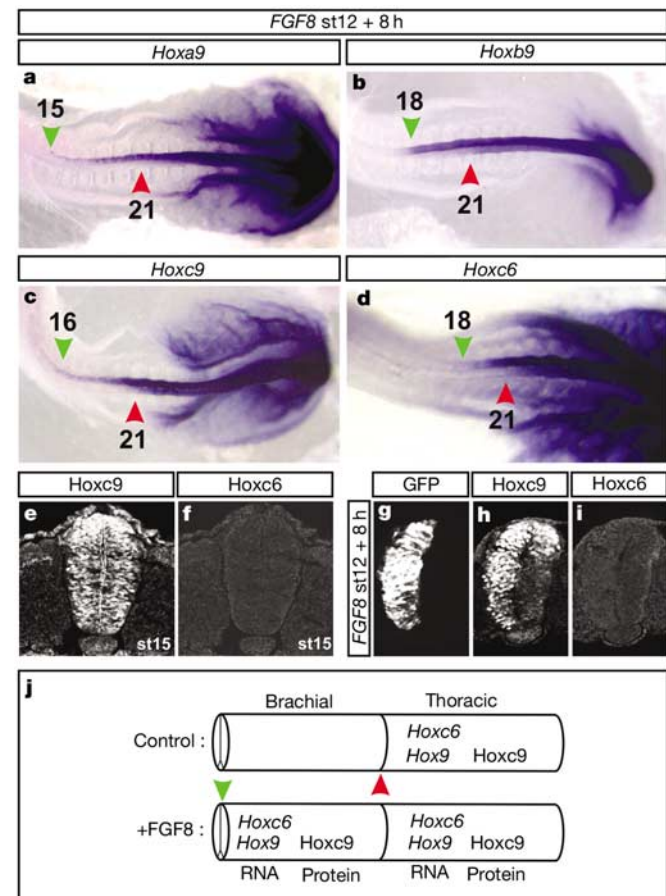


Figure 4 Rapid repatterning of neural progenitor Hox profile after brachial *FGF8* expression. **a–d**, Rostral expansion in domains of expression of *Hox9* paralogues and of *Hoxc6*, 8 h after unilateral *FGF8* electroporation. Red arrowhead indicates normal rostral expression boundary, green arrowhead indicates rostral boundary after exposure to *FGF8*. **e, f**, Expression of *Hoxc9* and absence of *Hoxc6* protein in stage 15 thoracic neural tube. **g–i**, Ectopic brachial expression of *Hoxc9* protein, but not *Hoxc6* protein, 8 h after *FGF8* electroporation in stage 12 neural tube. The restriction of the repressive activity of *Hox9* proteins to post-mitotic neurons could reflect gating of Hox activities by co-factors such as *Meis*/*Pbx* proteins⁴⁶, a possibility supported by the restricted expression of *Meis1* and *Pbx3* in MNs (J.S.D and T.M.J., unpublished observations). **j**, Schematic of *Hox6* and *Hox9* mRNA and protein in brachial and thoracic neural tube in normal and *FGF8*-exposed embryos. A mismatch in *Hoxc6* mRNA and protein has also been reported in the chick limb⁴⁷, suggesting a more general constraint on *Hoxc6* expression. By analogy with other *Hox* genes⁴⁸, this regulation may involve post-transcriptional regulatory controls.

expression at stage 12 and analysis 8 h later, ectopic rostral expression of *Hoxa9*, *Hoxb9*, and *Hoxc9* mRNAs and *Hoxc9* protein was detected within neural progenitors (Fig. 4a–c, g, h). Expression of *FGF8* also resulted in a rostral expansion in the domain of *Hoxc6* mRNA expression (Fig. 4d), although *Hoxc6* protein was still not detected (Fig. 4i). The pattern of *Hoxc6* and *Hox9* expression in thoracic progenitors was not markedly altered by *FGF8* expression (Fig. 4a–c). Moreover, expression of *FGF8* at stage 17, after the onset of MN differentiation, did not alter the profile of Hox-c expression (Supplementary Fig. S4h–k). Together, these findings indicate that exposure of brachial progenitors to FGF8 rapidly induces *Hoxc9* expression, in the absence of *Hoxc6* protein, thus establishing a Hox profile characteristic of thoracic level progenitors (Fig. 4j).

Hox-c activities in post-mitotic MNs

The difference in the time of onset of *Hox6* and *Hox9* protein expression at brachial and thoracic levels led us to examine when the activity of these two Hox paralogue groups is required for MN columnar specification. To address this issue, we examined whether MN columnar identity can be respecified by selective expression of Hox proteins in post-mitotic MNs. To restrict Hox protein expression, we used a 9-kilobase (kb) 5' flanking region of the mouse *Hb9* gene, which confers expression to post-mitotic neurons and excludes expression from progenitor cells^{18,24}.

Expression of *Hoxc9* in post-mitotic brachial MNs suppressed *Hoxc6* expression and blocked the differentiation of *RALDH2*⁺ LMC neurons, and of *Isl2*⁺, *Lim1*⁺ lateral LMC neurons (Fig. 5a–c and data not shown). However, post-mitotic *Hoxc9* expression failed to induce CT differentiation, as revealed by the lack of *BMP5* expression,

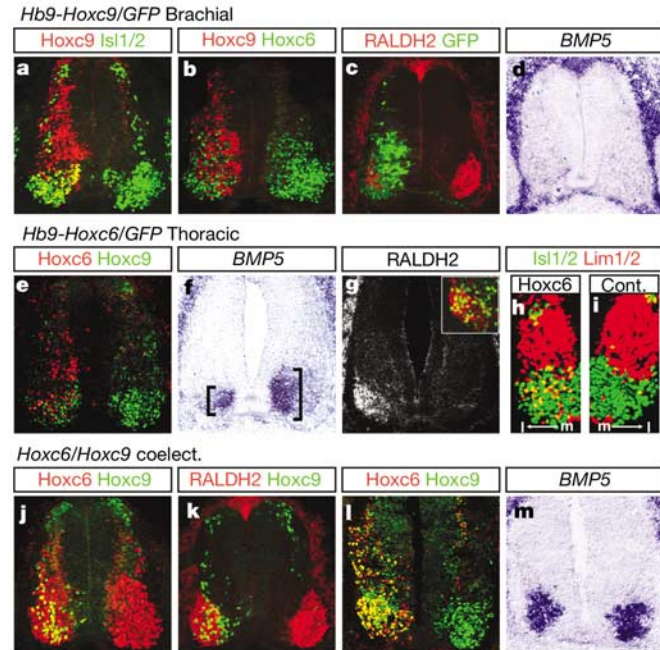


Figure 5 Activities of *Hoxc6* and *Hoxc9* in post-mitotic neurons. **a**, Expression of *Hb9-Hoxc9/GFP* at brachial levels results in many neurons that co-express *Isl1/2* and *Hoxc9*. Even though the *Hb9* promoter occasionally results in ectopic Hox expression in interneurons as well as MNs, no expression is detected in progenitor cells. **b, c**, Loss of *Hoxc6* and *RALDH2* expression after brachial post-mitotic expression of *Hoxc9*. **d**, Expression of *Hoxc9* in brachial MNs does not induce *BMP5* expression. **e, f**, Repression of *Hoxc9* and *BMP5* expression after post-mitotic thoracic expression of *Hoxc6*. **g–i**, Expression of *Hoxc6* in thoracic MNs induces expression of *RALDH2* and co-expression of *Isl2* and *Lim1*. Inset in **g** indicates co-expression of *Hoxc6* (green) and *RALDH2* (red). **j–m**, Effect of *Hoxc6* and *Hoxc9* co-expression at brachial (**j, k**) and thoracic (**l, m**) levels.

and of dorsomedially located *Hoxc9*⁺, *Isl1*⁺ MNs (Fig. 5a, d and data not shown). These findings provide evidence that *Hoxc9* function is required in brachial progenitors as well as post-mitotic MNs for the ectopic specification of CT identity.

Conversely, expression of *Hoxc6* in post-mitotic thoracic MNs repressed *Hoxc9* expression and prevented the expression of *BMP5* by thoracic MNs (Fig. 5e, f). But in addition, post-mitotic *Hoxc6* expression induced expression of *RALDH2*⁺ LMC neurons, and *Isl2*⁺, *Lim1*⁺ lateral LMC neurons (Fig. 5g–i). Thus, *Hoxc6* can specify brachial LMC identity solely through actions in post-mitotic MNs.

To examine whether the post-mitotic blockade of LMC differentiation by *Hoxc9*, and of CT differentiation by *Hoxc6*, depends primarily on repression of the complementary Hox-c protein, we assayed the consequences of forced co-expression of *Hoxc6* and *Hoxc9* at brachial and thoracic levels. At brachial levels, many MNs that expressed *Hoxc9* also expressed *RALDH2* (Fig. 5j, k), and at thoracic levels *BMP5* expression was preserved, despite widespread expression of *Hoxc6* (Fig. 5l, m). These findings provide evidence that the ability of *Hoxc9* to block LMC differentiation, and of *Hoxc6* to block CT differentiation, is mediated primarily through repression of their complementary Hox proteins.

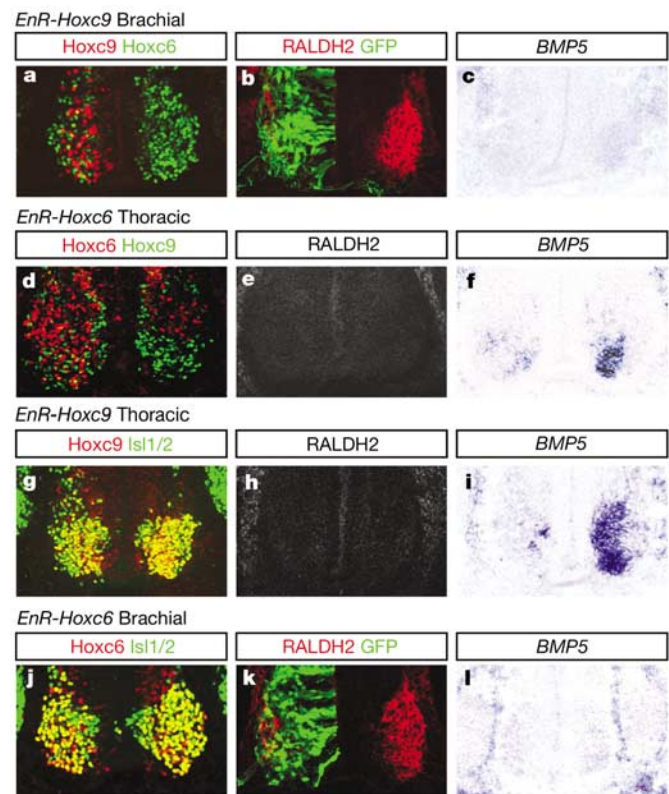


Figure 6 Actions of Engrailed repressor derivatives of *Hoxc6* and *Hoxc9* on columnar differentiation. **a–c**, Expression of *EnR-Hoxc9/GFP* in brachial neural tube represses *Hoxc6* and *RALDH2* expression, but fails to induce *BMP5* expression. **d–f**, Expression of *EnR-Hoxc6/GFP* at thoracic levels of the neural tube represses *Hoxc9* and *BMP5* expression, but fails to induce expression of *RALDH2*. We detected an increase in the proportion of MNs that expressed *Lim3* (data not shown), however, raising the possibility that some MNs have acquired a medial MMC-like character. **g–i**, Expression of *EnR-Hoxc9/GFP* in thoracic neural tube permits the generation of *Hoxc9*⁺, *Isl1/2*⁺ MN, but these neurons do not express *BMP5* or *RALDH2*. **j–l**, Expression of *EnR-Hoxc6/GFP* in brachial neural tube permits the generation of *Hoxc6*⁺, *Isl1/2*⁺ MNs, but these neurons do not express *BMP5* or *RALDH2*. Expression of *VP16-Hoxc6* and *VP16-Hoxc9* fusion proteins appear to function in a manner similar to their wild-type counterparts, a finding that parallels observations of Hox activity in *Drosophila*⁴⁹.

Requirement for Hox-c activity in MN columnar specification

Hox proteins appear to specify MN columnar identity through mutual cross-repressive interactions as well as the induction of columnar differentiation markers, posing the question of whether Hox proteins function as repressors and/or activators. To address this issue, we generated presumed repressor derivatives of Hoxc6 and Hoxc9 by fusing full-length Hox-c coding regions to the repressor domain (EnR) of the *Drosophila* Engrailed protein²⁵. Expression of *EnR-Hoxc9* under *pCAGGS* control in the stage 12 brachial neural tube suppressed Hoxc6 expression and the differentiation of RALDH2⁺ LMC neurons, but failed to induce *BMP5* expression in MNs (Fig. 6a–c). Conversely, thoracic expression of *EnR-Hoxc6* under *pCAGGS* control suppressed Hoxc9 expression and the differentiation of *BMP5*⁺ CT neurons, but failed to induce RALDH2 expression (Fig. 6d–f). As a specificity control, expression of *EnR-Hoxc8* at brachial levels repressed Hoxc5 at rostral brachial levels but did not repress Hoxc6 expression or the differentiation of LMC neurons (Supplementary Fig. S7a–c). These findings suggest that the cross-repressive interactions of Hoxc9 and Hoxc6 reflect transcriptional repressor activities, whereas Hox activator functions are required for ectopic induction of columnar differentiation markers.

The apparent requirement for Hox activator function in columnar differentiation raises the issue of whether the EnR Hox-c derivatives inhibit LMC and CT differentiation within the normal domains of Hoxc6 and Hoxc9 expression. Thoracic expression of *EnR-Hoxc9* blocked the expression of *BMP5* in thoracic MNs, and prevented the later dorsomedial migration of MNs (Fig. 6g–i and data not shown). Conversely, brachial expression of *EnR-Hoxc6* blocked the differentiation of RALDH2⁺ LMC neurons (Fig. 6j–l). Thus, the loss of both LMC and CT columnar identity after *EnR-Hoxc6* or

EnR-Hoxc9 expression leaves most brachial and thoracic Isl1/2⁺ MNs without an appropriate columnar character, although their precise subtype identity remains to be established. Together, these data provide evidence that Hox6 and Hox9 activities are normally required for the specification of LMC and CT columnar identities at brachial and thoracic levels of the spinal cord.

Discussion

Hox function and MN columnar specification

Our findings reveal that the specification of MN columnar subtypes along the rostrocaudal axis of the spinal cord involves sequential phases of Hox expression and activity in progenitor cells and post-mitotic MNs (Fig. 7a). The positional identity of progenitor cells at brachial and thoracic levels is reflected in the status of Hox9 expression: brachial progenitors lack Hox9 protein expression, whereas thoracic progenitors express Hox9 proteins. Expression of Hox9 proteins by thoracic progenitors anticipates the expression of Hox9 proteins by thoracic MNs, and the absence of Hox9 protein expression provides a brachial progenitor context that permits the onset of Hox6 protein expression in post-mitotic brachial MNs. Nevertheless, our findings do not exclude the possibility that other Hox proteins contribute to brachial progenitor identity. The differentiation of brachial LMC neurons has been shown to depend on retinoid signals provided by the paraxial mesoderm^{10,26}. Thus, Hoxc6 expression and brachial LMC differentiation may depend both on an early progenitor Hox profile, and on a post-mitotic phase of retinoid signalling from the paraxial mesoderm.

The profile of Hox protein expression by post-mitotic MNs appears to be a major determinant of their columnar fate (Fig. 7a). Post-mitotic brachial misexpression of Hoxc9 inhibits LMC identity but is insufficient to direct CT identity, suggesting that sequential phases of Hoxc9 expression by thoracic progenitors and post-mitotic MNs are necessary for CT identity. In contrast, Hoxc6 appears able to function as a post-mitotic determinant of brachial LMC identity. Furthermore, the ability of EnR Hox derivatives to inhibit brachial LMC and CT differentiation provides the best evidence so far^{27–30} that Hox6 and Hox9 activities are required normally for MN columnar specification.

LMC neurons are generated at lumbar as well as brachial levels of the spinal cord, raising the issue of whether FGF signalling and Hox proteins have a more general role in the specification of LMC identity. *Hox10* paralogues are expressed by lumbar level LMC neurons^{31,32} and are regulated by signals from the node³¹ through the synergistic activities of FGFs and GDF11¹¹. Moreover, ectopic thoracic expression of *Hoxd10* induces RALDH2 expression in MNs (J.S.D. and T.M.J., unpublished data), supporting the idea that Hox proteins are involved in the specification of both lumbar and brachial LMC identity.

Comparative strategies of Hox function

The principles of homeodomain protein function along the rostrocaudal axis parallel those that operate along the dorsoventral axis to establish generic MN identity^{3,4}. Along both axes, the initial graded activity of a secreted signalling factor establishes broad domains of homeodomain protein expression that are refined through selective cross-repressive interactions. These two intersecting programmes of transcriptional cross-repression, however, appear to act at different stages of MN specification. Dorsoventrally, homeodomain cross-repressive interactions are evident within neural progenitor cells^{33,34}, whereas rostrocaudally Hox cross-repressive interactions occur within post-mitotic MNs. Nevertheless, the convergence of these two patterning programmes ensures that expression of RALDH2, *BMP5* and other Hox-directed features of columnar differentiation is confined to MNs.

Our findings in the spinal cord can be compared with studies on the role of *Hox* genes in the specification of MN identity in the hindbrain. Most compellingly, Hoxb1 has been shown to control the

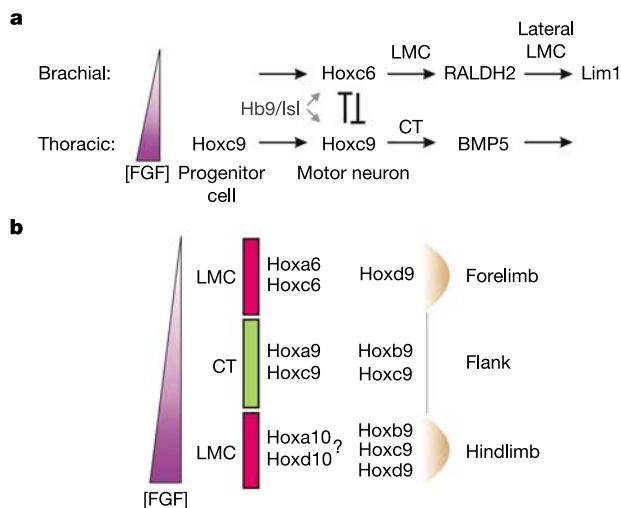


Figure 7 Hox6 and Hox9 activities in motor neuron columnar differentiation and topography. **a**, Model indicating the roles of FGF signalling and Hox6 and Hox9 expression in the specification of MN columnar identity. Hoxc9 expression in progenitors and cross-repressive interactions between Hox6 and Hox9 proteins in post-mitotic Hb9⁺, Isl1⁺ MNs consolidate the distinct Hox profiles of LMC and CT neurons. Hox6 activity in brachial MNs directs RALDH2 expression and late features of LMC identity, whereas Hox9 activity in thoracic MNs directs *BMP5* expression and the dorsomedial migration of MNs. **b**, Hox expression and the register between the rostrocaudal positions of LMC and limb formation. Model suggests how exposure of neural and lateral plate mesodermal cells to a common node-derived source of FGFs could establish distinct *Hox* expression profiles in these two tissues, directing LMC and limb formation in an aligned manner. The profiles of Hox expression in lumbar LMC neurons and lateral plate mesoderm are inferred from refs 41 and 44.

differentiation of facial MNs^{13,14,35}, through both cell autonomous and non-autonomous outputs³⁶. It remains unclear, however, whether Hoxb1 controls MN specification through its activity in progenitor cells and/or post-mitotic MNs. And whether the combined activator and repressor roles suggested for individual Hox proteins in spinal MN columnar specification has a parallel in Hox function in the hindbrain remains to be determined.

The emerging logic of Hox function in spinal MN columnar diversification contrasts with certain features of *HOMC/Hox* function in rostrocaudal patterning in the *Drosophila* embryo and vertebrate hindbrain. In both systems, the actions of more posteriorly expressed *Hox* genes typically dominate over those of more anteriorly expressed genes—a phenomenon termed “posterior prevalence”^{37,38}. Our findings argue against a simple posterior prevalence of Hox function in post-mitotic MN specification, because ectopic caudal expression of Hoxc6 is as effective as ectopic rostral expression of Hoxc9. Exceptions to the posterior prevalence rule of Hox function have been reported in both *Drosophila* and vertebrate embryos^{37,39}, suggesting that tissue context influences the logic of Hox function.

Hox function and MN topographic organization

Our findings also provide insights into the role of Hox proteins in establishing the topographic organization of spinal MNs and their peripheral targets. One aspect of such topography is a register between the rostrocaudal positions of the LMC in the spinal cord, and of the limb field in the lateral plate mesoderm. The pathway of LMC specification revealed here has an intriguing counterpart in the proposed functions of FGFs and Hox proteins in determining limb position. Local application of FGFs to thoracic mesoderm induces the formation of an additional limb in place of body-wall mesoderm⁴⁰. Moreover, exposure of lateral plate mesoderm to FGFs induces an early switch in the rostrocaudal profile of *Hox9* paralog expression⁴¹. Thus, exposure of neural and lateral plate mesodermal cells to a common node-derived source of FGFs could establish distinct profiles of *Hox* gene expression in these two tissues, profiles that in turn direct the alignment of LMC and limb formation (Fig. 7b).

Once the register between LMC neurons and limb targets has been established, the expression of Hox proteins by MNs appears to initiate more refined aspects of MN topography. The assignment of brachial LMC identity by Hox6 proteins results in the expression of RALDH2, establishing the LMC as a local source of retinoids²⁰. In turn, exposure of LMC neurons to retinoids induces the patterned expression of LIM homeodomain proteins that links MN position in the spinal cord to motor axon trajectory along the dorsoventral axis of the limb^{20,42}. Thus, the expression of Hox6 by brachial MNs initially establishes the rostrocaudal position of LMC generation, and subsequently directs dorsoventral motor topography. Conversely, the ectopic expression of Hoxc9 in brachial level MNs is associated with the redirection of their axons to sympathetic ganglion targets, an axonal trajectory characteristic of CT neurons (Supplementary Fig. S8a–d). Because the specification of CT identity by Hox9 proteins is accompanied by *BMP5* expression, it is possible that BMPs influence aspects of CT differentiation in a manner similar to the role of RALDH2 expression and retinoid signalling in LMC differentiation.

Could Hox proteins have further roles in MN diversification and topography? Within the LMC, MNs can be further subdivided into discrete pools, each destined to innervate a single muscle target in the limb⁵. The differential rostrocaudal domains of expression of the Hoxc5–Hoxc8 protein pair parallel motor pool position within the brachial LMC⁴³ (J.D. and T. J., unpublished data), and later profiles of *Hox* gene expression are also indicative of motor pool restriction^{10,31,32}. Although the targeted inactivation of *Hoxc8*, *Hoxa10* and *Hoxd10* in mice causes defects in motor axon projections in the limb^{44,45}, the cellular basis of these defects remains unclear. Our

findings raise the possibility that MN columnar and pool identities, and consequent patterns of motor innervation in the limb, are established through the selective activities of complementary homeodomain protein pairs embedded within individual *Hox* clusters. □

Methods

Expression constructs

For expression of *FGF8*, the murine complementary DNA was cloned into the *pCMV* cytomegalovirus (*CMV*)-based expression vector. Full-length *Hox* cDNAs were obtained by RT-PCR of embryonic day (E)10.5–E12.5 mouse or stage (st)25–st27 chick embryo total RNA using the One-Step RT-PCR kit (Invitrogen) and were confirmed by DNA sequencing. The mouse *Hoxc6* cDNA corresponded to the longer P_{RII} transcript. cDNAs were cloned into *pCAGGS* or *pHb9* vectors by standard procedures. For generation of *Drosophila* EnR (amino acids 2–229) derivatives, cDNAs were cloned by PCR to generate in-frame fusion proteins.

In ovo electroporation

Electroporation was performed as described¹⁸. Results shown for each experiment are representative of at least eight electroporated embryos. For misexpression of Hox-c proteins in chick embryos, plasmids were titrated to achieve levels of protein expression qualitatively similar to endogenous levels. Typically this was in the range of 100–500 µg µl⁻¹ for the *pCAGGS* vector and 3–4 ng µl⁻¹ for the *Hb9* vector, using *CMV/GFP* or *Hb9/GFP* plasmids as carrier DNA. Similarly, the *CMV/FGF8* plasmid was titrated to a level (between 100–200 ng µl⁻¹) where somite and dorsoventral patterning and generic aspects of MN generation were unaffected.

In situ hybridization histochemistry and immunohistochemistry

In situ hybridization was performed as described¹⁷. Chick probes for analysis of *Hoxc6*, *Hoxc9*, *Hoxa9*, *Hoxb9* and *Hoxd9* expression were provided by C. Tabin. Probes against *Hoxa6* and *Hoxb6* were obtained by RT-PCR, using sequence information obtained from the chick EST data consortium. Antibodies against Hox-c proteins and LIM homeodomain proteins were used as previously described^{11,17}. Additional antibodies were obtained as follows: goat anti-Hoxa9 (Santa Cruz Biotechnology, SC-17155), mouse anti-phospho MAPK (Sigma, M8159).

Received 22 July; accepted 3 September 2003; doi:10.1038/nature02051.

1. Mountcastle, V. B. The columnar organization of the neocortex. *Brain* **120**, 701–722 (1997).
2. Sanders, T. A., Lumsden, A. & Ragsdale, C. W. Arcuate plan of chick midbrain development. *J. Neurosci.* **22**, 10742–10750 (2002).
3. Jessell, T. M. Neuronal specification in the spinal cord: inductive signals and transcriptional codes. *Nature Rev. Genet.* **1**, 20–29 (2000).
4. Briscoe, J. & Ericson, J. Specification of neuronal fates in the ventral neural tube. *Curr. Opin. Neurobiol.* **11**, 43–49 (2001).
5. Landmesser, L. The distribution of motoneurons supplying chick hind limb muscles. *J. Physiol. (Lond.)* **284**, 371–389 (1978).
6. Hollyday, M. Organization of motor pools in the chick lumbar lateral motor column. *J. Comp. Neurol.* **194**, 143–170 (1980).
7. Hollyday, M. Motoneuron histogenesis and the development of limb innervation. *Curr. Top. Dev. Biol.* **15**, 181–215 (1980).
8. Gutman, C. R., Ajmera, M. K. & Hollyday, M. Organization of motor pools supplying axial muscles in the chicken. *Brain Res.* **609**, 129–136 (1993).
9. Shirasaki, R. & Pfaff, S. L. Transcriptional codes and the control of neuronal identity. *Annu. Rev. Neurosci.* **25**, 251–281 (2002).
10. Ensini, M., Tsuchida, T. N., Belting, H. G. & Jessell, T. M. The control of rostrocaudal pattern in the developing spinal cord: specification of motor neuron subtype identity is initiated by signals from paraxial mesoderm. *Development* **125**, 969–982 (1998).
11. Liu, J. P., Laufer, E. & Jessell, T. M. Assigning the positional identity of spinal motor neurons: rostrocaudal patterning of Hox-c expression by FGFs, Gdf11, and retinoids. *Neuron* **32**, 997–1012 (2001).
12. Bel-Vialar, S., Itasaki, N. & Krumlauf, R. Initiating Hox gene expression: in the early chick neural tube differential sensitivity to FGF and RA signaling subdivides the HoxB genes in two distinct groups. *Development* **129**, 5103–5115 (2002).
13. Studer, M., Lumsden, A., Ariza-McNaughton, L., Bradley, A. & Krumlauf, R. Altered segmental identity and abnormal migration of motor neurons in mice lacking Hoxb-1. *Nature* **384**, 630–634 (1996).
14. Bell, E., Wingate, R. J. & Lumsden, A. Homeotic transformation of rhombomere identity after localized Hoxb1 misexpression. *Science* **284**, 2168–2171 (1999).
15. Rossel, M. & Capecci, M. R. Mice mutant for both Hoxa1 and Hoxb1 show extensive remodeling of the hindbrain and defects in craniofacial development. *Development* **126**, 5027–5040 (1999).
16. Prasad, A. & Hollyday, M. Development and migration of avian sympathetic preganglionic neurons. *J. Comp. Neurol.* **307**, 237–258 (1991).
17. Tsuchida, T. et al. Topographic organization of embryonic motor neurons defined by expression of LIM homeobox genes. *Cell* **79**, 957–970 (1994).
18. William, C. M., Tanabe, Y. & Jessell, T. M. Regulation of motor neuron subtype identity by repressor activity of Mnx class homeodomain proteins. *Development* **130**, 1523–1536 (2003).
19. Niederreither, K., McCaffery, P., Drager, U. C., Chambon, P. & Dolle, P. Restricted expression and retinoic acid-induced downregulation of the retinaldehyde dehydrogenase type 2 (RALDH-2) gene during mouse development. *Mech. Dev.* **62**, 67–78 (1997).
20. Sockanathan, S. & Jessell, T. M. Motor neuron-derived retinoid signaling specifies the subtype identity of spinal motor neurons. *Cell* **94**, 503–514 (1998).

21. Hart, K. C. *et al.* Transformation and Stat activation by derivatives of FGFR1, FGFR3, and FGFR4. *Oncogene* **19**, 3309–3320 (2000).
22. Gabay, L., Seger, R. & Shilo, B. Z. MAP kinase in situ activation atlas during *Drosophila* embryogenesis. *Development* **124**, 3535–3541 (1997).
23. Cai, J. *et al.* Evidence for the differential regulation of Nkx-6.1 expression in the ventral spinal cord and foregut by Shh-dependent and -independent mechanisms. *Genesis* **27**, 6–11 (2000).
24. Arber, S. *et al.* Requirement for the homeobox gene Hb9 in the consolidation of motor neuron identity. *Neuron* **23**, 659–674 (1999).
25. Jaynes, J. B. & O'Farrell, P. H. Active repression of transcription by the engrailed homeodomain protein. *EMBO J.* **10**, 1427–1433 (1991).
26. Sockanathan, S., Perlmann, T. & Jessell, T. M. Retinoid receptor signaling in postmitotic motor neurons regulates rostrocaudal positional identity and axonal projection pattern. *Neuron* **40**, 97–111 (2003).
27. Kostic, D. & Capecchi, M. R. Targeted disruptions of the murine Hoxa-4 and Hoxa-6 genes result in homeotic transformations of components of the vertebral column. *Mech. Dev.* **46**, 231–247 (1994).
28. Garcia-Gasca, A. & Spyropoulos, D. D. Differential mammary morphogenesis along the anteroposterior axis in Hoxc6 gene targeted mice. *Dev. Dyn.* **219**, 261–276 (2000).
29. Chen, F. & Capecchi, M. R. Hoxa9, Hoxb9, and Hoxd9, function together to control development of the mammary gland in response to pregnancy. *Proc. Natl Acad. Sci. USA* **96**, 541–546 (1999).
30. Suemori, H. & Noguchi, S. Hox C cluster genes are dispensable for overall body plan of mouse embryonic development. *Dev. Biol.* **220**, 333–342 (2000).
31. Lance-Jones, C., Omelchenko, N., Bailis, A., Lynch, S. & Sharma, K. Hoxd10 induction and regionalization in the developing lumbosacral spinal cord. *Development* **128**, 2255–2268 (2001).
32. Carpenter, E. M. Hox genes and spinal cord development. *Dev. Neurosci.* **24**, 24–34 (2002).
33. Briscoe, J., Pierani, A., Jessell, T. M. & Ericson, J. A homeodomain protein code specifies progenitor cell identity and neuronal fate in the ventral neural tube. *Cell* **101**, 435–445 (2000).
34. Muhr, J., Andersson, E., Persson, M., Jessell, T. M. & Ericson, J. Groucho-mediated transcriptional repression establishes progenitor cell pattern and neuronal fate in the ventral neural tube. *Cell* **104**, 861–873 (2001).
35. Goddard, J. M., Rossel, M., Manley, N. R. & Capecchi, M. R. Mice with targeted disruption of Hoxb-1 fail to form the motor nucleus of the VIIth nerve. *Development* **122**, 3217–3228 (1996).
36. Cooper, K. L., Leisenring, W. M. & Moens, C. B. Autonomous and nonautonomous functions for Hox/Pbx in branchiomotor neuron development. *Dev. Biol.* **253**, 200–213 (2003).
37. Duboule, D. & Morata, G. Colinearity and functional hierarchy among genes of the homeotic complexes. *Trends Genet.* **10**, 358–364 (1994).
38. Kmita, M. & Duboule, D. Organizing axes in time and space; 25 years of colinear tinkering. *Science* **301**, 331–333 (2003).
39. Jegalian, B. G. & De Robertis, E. M. Homeotic transformations in the mouse induced by overexpression of a human Hox3.3 transgene. *Cell* **71**, 901–910 (1992).
40. Cohn, M. J., Izpisua-Belmonte, J. C., Abud, H., Heath, J. K. & Tickle, C. Fibroblast growth factors induce additional limb development from the flank of chick embryos. *Cell* **80**, 739–746 (1995).
41. Cohn, M. J. *et al.* Hox9 genes and vertebrate limb specification. *Nature* **387**, 97–101 (1997).
42. Kania, A. & Jessell, T. M. Topographic motor projections in the limb imposed by LIM homeodomain protein regulation of ephrin-A:EphA interactions. *Neuron* **38**, 581–596 (2003).
43. Hollyday, M. & Jacobson, R. D. Location of motor pools innervating chick wing. *J. Comp. Neurol.* **302**, 575–588 (1990).
44. Wahba, G. M., Hostikka, S. L. & Carpenter, E. M. The paralogous Hox genes Hoxa10 and Hoxd10 interact to pattern the mouse hindlimb peripheral nervous system and skeleton. *Dev. Biol.* **231**, 87–102 (2001).
45. Tiret, L., Le Mouellie, H., Maury, M. & Brulet, P. Increased apoptosis of motoneurons and altered somatotopic maps in the brachial spinal cord of Hoxc-8-deficient mice. *Development* **125**, 279–291 (1998).
46. Mann, R. S. & Affolter, M. Hox proteins meet more partners. *Curr. Opin. Genet. Dev.* **8**, 423–429 (1998).
47. Nelson, C. E. *et al.* Analysis of Hox gene expression in the chick limb bud. *Development* **122**, 1449–1466 (1996).
48. Brend, T., Gilthorpe, J., Summerbell, D. & Rigby, P. W. Multiple levels of transcriptional and post-transcriptional regulation are required to define the domain of Hoxb4 expression. *Development* **130**, 2717–2728 (2003).
49. Li, X. & McGinnis, W. Activity regulation of Hox proteins, a mechanism for altering functional specificity in development and evolution. *Proc. Natl Acad. Sci. USA* **96**, 6802–6807 (1999).

Supplementary Information accompanies the paper on www.nature.com/nature.

Acknowledgements We thank F. Lo for technical assistance; C. Tabin for chick *Hox in situ* probes; and E. Laufer for advice and critical reagents. We thank R. Axel, J. DeNooij, J. Ericson, E. Laufer, R. Mann, B. Novitsch and S. Wilson for comments, and K. MacArthur for help in preparing the manuscript. J.-P.L. is supported by a grant from NINDS and is a recipient of a Burroughs Wellcome Fund Career Award in Biomedical Sciences. J.D. is a research associate and T.M.J. an investigator of the Howard Hughes Medical Institute.

Competing interests statement The authors declare that they have no competing financial interests.

Correspondence and requests for materials should be addressed to T.M.J. (tmj1@columbia.edu) or J.S.D. (jd2009@columbia.edu).